Since January 2020 Elsevier has created a COVID-19 resource centre with free information in English and Mandarin on the novel coronavirus COVID-19. The COVID-19 resource centre is hosted on Elsevier Connect, the company's public news and information website.

Materials Science & Engineering C 118 (2021) 111441

Contents lists available at ScienceDirect

Materials Science & Engineering C

journal homepage: www.elsevier.com/locate/msec

Evaluation of remodeling and regeneration of electrospun PCL/fibrin vascular grafts in vivo

Liang Zhao[a,b,*,1], Xiafei Li[c,1], Lei Yang[a,d,1], Lulu Sun[a], Songfeng Mu[a,d], Haibin Zong[c], Qiong Li[e], Fengyao Wang[f], Shuang Song[a], Chengqiang Yang[a], Changhong Zhao[a], Hongli Chen[a], Rui Zhang[g], Shicheng Wang[h], Yuzhen Dong[d,**], Qiqing Zhang[a,**]

[a] College of Life Science and Technology, Xinxiang Medical University, Xinxiang, China
[b] Key Laboratory of Cardiac Structure Research, Zhengzhou Seventh People's Hospital, Zhengzhou, China
[c] College of Medical Engineering, Xinxiang Medical University, Xinxiang, China
[d] First Affiliated Hospital, Xinxiang Medical University, Xinxiang, China
[e] Nursing School, Xinxiang Medical University, Xinxiang, China
[f] The First Affiliated Hospital, Henan University of Science and Technology, Luoyang, China
[g] Service Center for Transformation of Scientific and Technological Achievements, Xinxiang Medical University, Xinxiang, China
[h] General Surgery Department, West District Hospital of Nanyang The First People's Hospital, Nanyang, China

ARTICLE INFO

Keywords:
PCL/fibrin vascular grafts
Electrospinning
Tissue remodeling and regeneration
In vivo
Inflammatory cytokines

ABSTRACT

The success of artificial vascular graft in the host to obtain functional tissue regeneration and remodeling is a great challenge in the field of small diameter tissue engineering blood vessels. In our previous work, poly(ε-caprolactone) (PCL)/fibrin vascular grafts were fabricated by electrospinning. It was proved that the PCL/fibrin vascular graft was a suitable small diameter tissue engineering vascular scaffold with good biomechanical properties and cell compatibility. Here we mainly examined the performance of PCL/fibrin vascular graft in vivo. The graft showed randomly arranged nanofiber structure, excellent mechanical strength, higher compliance and degradation properties. At 9 months after implantation in the rat abdominal aorta, the graft induced the regeneration of neoarteries, and promoted ECM deposition and rapid endothelialization. More importantly, the PCL/fibrin vascular graft showed more microvessels density and fewer calcification areas at 3 months, which was beneficial to improve cell infiltration and proliferation. Moreover, the ratio of M2/M1macrophage in PCL/fibrin graft had a higher expression level and the secretion amount of pro-inflammatory cytokines started to increase, and then decreased to similar to the native artery. Thus, the electrospun PCL/fibrin tubular vascular graft had great potential to become a new type of artificial blood vessel scaffold that can be implanted in vivo for long term.

1. Introduction

Cardiovascular disease (CVD) is one of the killers that seriously threaten human health. CVD has a mortality rate of 31.7% worldwide and accounts for 50% of deaths from noncommunicable diseases [1]. Particularly, CVD causes 80% of deaths in low- and middle-income countries and is the most important cause of death [2]. Up to now, there are many ways to deal with CVD, but coronary artery bypass surgery is still generally recognized as the most effective treatment. Currently the main sources of vascular grafts are from great saphenous vein of patient himself. Although autologous vascular grafts exhibit good biocompatibility, non-immune response, non-toxicity and ease of growth, the patient's individual donor tissue is often insufficient to meet clinical needs [3]. Thus, the artificial vascular instead of the autologous blood vessels are the best choice and have potential application for the treatment of CVD.

In the past few years, three kinds of synthetic materials including expanded polytetrafluoroethylene (ePTFE), polyethylene terephthalate (Dacron) and polyurethane (PU) have been successfully applied to clinical treatment as large diameter (inner diameter > 6 mm) artificial vascular grafts [4,5]. Unfortunately, synthetic grafts still face many challenges that we need to overcome, such as prone to thrombosis,

* Correspondence to: L. Zhao, College of Life Science and Technology, Xinxiang Medical University, Xinxiang, China.
** Corresponding authors.
E-mail addresses: zhaoliang4321@163.com (L. Zhao), dongyuzhen1998@163.com (Y. Dong), zhangqiq@126.com (Q. Zhang).
[1] These authors contributed equally to this work.

https://doi.org/10.1016/j.msec.2020.111441
Received 22 April 2020; Received in revised form 16 August 2020; Accepted 21 August 2020
Available online 25 August 2020
0928-4931/

intimal hyperplasia, calcification and other complications [6,7].It is precisely these shortcomings that have limited the progress of small diameter (inner diameter < 6 mm) vascular grafts. Therefore, it is urgently needed to develop an artificial vascular graft with strong biomechanical properties, good compatibility, implantable and applicable to small diameter vascular remodeling, which will have a huge impact on the surgical management of CVD.

Tissue engineering technology offers hope for the construction of artificial vascular graft. Tissue engineered blood vessels include three major elements: scaffold material, growth factors and seed cells. Vascular scaffold material serves as a carrier of growth factors, and also provides a suitable microstructure environment for cell growth. So, constructing biologically active vascular scaffolds in vitro can promote vascular reconstruction and provide an exciting strategy for small diameter vascular grafting. The scaffold material should have certain biomechanical properties, which are an important index for vascular remodeling. Meanwhile, vascular graft should also have excellent flexibility, be resistant to kinking, and be easy to be sutured [8,9].Many researchers have confirmed that the mechanical properties of vascular scaffolds can regulate the function of macrophages, which has some definite effect on tissue remodeling [10,11]. Furthermore, it was found that mechanical stretching can greatly increase the proliferation of vascular smooth muscle cells (VSMCs), endothelial cells (ECs) and extracellular matrix (ECM) formation [12,13]. Therefore, we speculated that when vascular graft exhibits poor mechanical properties, it may delay vascular reconstruction.

In the process of vascular remodeling, cellular infiltration of vascular grafts is an important issue that requires urgent attention [14]. Researchers have been attempting to improve its performance. Agnieszka et al. [15] has compared different reseeding methods to define the most efficient technique enhancing recellularization of tissue engineered vascular vessels prior implantation. They found that puncturing of lyophilized tissue engineered vascular matrices could enhance the efficiency of their recellularization. In addition, domestic and foreign reports on the generation of functional artificial blood vessels in vivo are extremely rare. On the other hand, we are required to pay attention to the effect of immune response on graft vascular remodeling in vivo [16]. Although some graft vascular scaffold materials has excellent mechanical properties, they lack the function of vascular remodeling and easily cause chronic inflammatory reactions [17]. At the same time, researchers found that some two or more different materials combined into a composite material can cause calcification when implanted as vascular graft [18]. The series of problems we have described above often occurring to vascular tissue engineering grafts.

In the previous work, we successfully prepared the PCL/fibrin vascular scaffold through electrospinning technology, and found that it had good biomechanical properties, cell compatibility, biocompatibility and degradation properties [19].Experiments results have confirmed that the PCL/fibrin scaffold material can be an ideal scaffold material for small diameter tissue engineering blood vessels. So we hypothesize that PCL/fibrin vascular scaffold is suitable as a substitute for artificial blood vessels in vivo. To verify this hypothesis, in this paper, the PCL/fibrin vascular scaffold was implanted into the abdominal aorta model at 1, 3, and 9 months to assess the mechanical properties, cell proliferation, formation and secretion of extracellular matrix, functional, immune response and calcifications characteristics of the grafts.

2. Materials and methods

2.1. Materials

PCL (Mn:80,000) was come from Sigma Aldrich Trading Co., Ltd. (Shanghai, China). Fibrin was acquired from Thermo Fisher. 98% formic acid, 5% fetal bovine serum, TritonX-100, monoclonal antibody secondary antibody and 4,6-diamidino-2-phenylindole (DAPI) were purchased from Jisi Instrument Equipment Co., Ltd. (Wuhan, China). 10%KCl, adrenaline, Ach, SNP, 4% paraformaldehyde, Masson staining kit, hematoxylin eosin staining kit, Safranin O, Verhoeffi-Van Gieson staining (VVG) and von Kossa staining kit were obtained from Sevier Biotechnology Co., Ltd. (Wuhan, China). Rabbit anti-von Willebrand factor (vWF) antibody, mouse monoclonal anti-CD31, mouse anti-α-SMA, anti-CD34 and mouse anti-SM-MHC were come from the Solarbio Co., Ltd. (Beijing, China). Mouse inflammatory factor ELISA detection kit was bought from Jianglai Biotechnology Co., Ltd. (Shanghai, China).

2.2. Fabrication of PCL/fibrin vascular scaffold

We have done large amount of similar work on the preparation of PCL/fibrin scaffolds by electrospinning technology [20–22]. In brief, PCL and fibrin at the weight of 20:80 were mixed thoroughly with 98% formic acid. At normal temperature, the solution was shaken and dissolved with thermostatic oscillator (HT-110X30, Shanghai, China) to prepare uniform and transparent PCL/fibrin polymer solution. A 20 mL syringe filled with PCL/ fibrin solution was set on the propeller. Before starting electrospinning equipment (FM1012, Dalian, China), the spinning parameters were set as voltage 20 kV, rotational speed 150 rpm/min, extrusion speed 1.5 mL/h, the spinning distance 10 cm. Then, under high electronic pressure, spinning solution solidified to form a tubular vascular scaffold. It was dried under the fume cabinet for 3 days to remove impurities from the vascular graft and stored at room temperature. Based on the parallel principles above, a control group PCL vascular graft also was prepared.

2.3. Observation of the scaffold morphology under scanning electron microscope

In order to facilitate sample observation, a tubular vascular graft was prepared into 1.5 mm (length) × 1.5 mm (width). The surface impurities were deleted out from the graft and then the graft was fixed on the double-sided adhesive conductive carbon film. It was placed on the sample platform of the ion sputtering apparatus for gold spraying for 30 s. The scanning electron microscope (Hitachi Model SU-8010, Japan) was set at an acceleration voltage of 12 kV, and pictures were collected and saved.

2.4. Implantation of the vascular graft

When a series of animal experimental operations were conducted, the rules of animal ethics protection and use and care about Xinxiang Medical University (Henan, China) should be strictly followed. The healthy SD male rats (n = 60, weight 200 g) were chosen and used from the laboratory animal center of Xinxiang Medical University. To prevent thrombosis, these rats should take aspirin anticoagulants orally before and after surgery. Meanwhile, the grafts to be implanted in rats should be sterilized. The process mainly included 2 h of ultraviolet irradiation, 1 h of immersion in 75% medical alcohol, and then repeated wash with 0.9% sodium chloride solution. Furthermore, surgical instruments had to be autoclaved in advance. All animal operations followed the principle of aseptic principle.

The rats were injected intraperitoneally with 5% chloral hydrate solution. After the anesthesia achieved the desired effect, the abdominal hair was removed, and then the rats were fixed on the experimental table. Then the surgical area was disinfected with iodophor and sterile hole towel was covered. To be more specific, we cut out 5 cm along the midline of the rat's abdomen, separated its organs in order, gently exposed the abdominal aorta, and then atraumatically clamped the proximal and distal ends of the blood vessels with microvascular forceps. We protected the peripheral nerve, blood vessels and internal organs, and cut off the main branch of the abdominal aorta about 2 cm long. By a magnifying glass, an 8-0 monofilament non-absorbent thread was used to anastomize the prepared vascular graft with the broken ends on both sides. The rat skin was sutured in succession of 2-0 silk

sutures and the incision was wrapped. Rats were sacrificed respectively after 1, 3 and 9 months of survival after transplantation. Again, it had to be stated that four rats died accidentally after transplantation in this experiment from some unknown cause. Survival rate was 93%.

2.5. Measurement of mechanical properties

In previous paper published by our research group, the measurement of mechanical properties such as maximum stress, elastic modulus and breaking strain have been reported in detail [19]. To test the mechanical strength of the vascular graft, it was cut into 3 mm (width) × 4 mm (length) × 0.3 mm (thickness) samples respectively and fixed on a microcomputer controlled electronic universal testing machine (Kesheng WWD-100D, Jinan, China) for measurement. Meanwhile, each sample needed to be tested three times repeatedly to calculate the average value and standard deviation of its elastic modulus, breaking strain and maximum stress.

Compliance is a key indicator for judging the success of vascular graft. SD rats were operated with ether drugs. After successful anesthesia, they were imaged on an ultra-high resolution small animal ultrasound instrument (Vevo3100, Canada). Furthermore, non-invasive blood pressure measuring instrument for tiny animals (NIBP200A, USA) was used to measure its systolic and diastolic blood pressure. The following formula was used to calculate its compliance.

$$\text{compliance per 100 mmHg (\%)} = \frac{(Rp2 - Rp1)/Rp2}{p1 - p2} \times 10^4$$

Among them, p1 and p2 respectively represent the measured values of high pressure and low pressure (mmHg). The inner diameter values of high and low pressure are indicated by Rp1 and Rp2.

2.6. Degradation of the graft in vivo

In order to better understand the condition of the graft, it was observed with a scanning electron microscope. In addition, we used gel permeation chromatography (HLC-8420GPC, Japan) to calculate the molecular weight. It should be noted that the sample should be strictly dust-removed before the measurement to reduce interference, and the tetrahydrofuran solvent should be selected to soak the samples for three days.

2.7. Detection of vascular function

To assess graft function, we used the aortic ring bioassay method. Briefly, a 4 mm long tubular graft was removed from the rat. The vascular graft was soaked in buffer for 2 h, after its surface adipose tissue was removed. The buffer needed to be changed every 20 min. At the same time, the addition of 10% KCl drugs (50 mM) stimulated vasoconstriction, which indicated the function of smooth muscle cells in the graft. In order to evaluate the relaxation function of vascular smooth muscle, we also added sodium nitroprusside (SNP, 0.9×10^{-7} mol/L) drugs. Vascular endothelium relaxed after adding acetylcholine (Ach, 9 μM) in pre-constricted segments by adrenaline (AD, 0.8 mM), suggesting the existence of endothelial cell function. Furthermore, it should be connected to the force sensor recording instrument (AD Instruments, Australia) to measure and retain the data.

2.8. Histology and immunofluorescence experiments

Vascular grafts were transplanted in vivo for 1 month, 3 months, and 9 months, respectively, and then SD rats were killed and samples (n = 4) were taken using excessive amount of anesthetics. The graft was prepared into a ring structure in turn, and observed and photographed under a stereo microscope (Xingming Optics, China). Samples were fixed with 4% paraformaldehyde and placed in a refrigerator at 4 °C for one day. Then, histological analysis experiments and SEM observation were performed respectively.

To better look at the morphology of the tubular graft, we used the SEM to inspect it. Before performing this test, the specimens should be fixed, dehydrated with different gradients of ethanol concentration sequentially and dried. Finally, the samples were sputter-coated with gold. Moreover, the graft should be dehydrated, soaked in wax, embedded, sectioned (thickness: 7 mm), baked, dewaxed, and rehydrated in sequence before performing histological analysis experiments. Subsequently, sections were stained using hematoxylin and eosin (H&E) staining kit, Masson staining kit, Safranin O, Verhoeff–van Gieson (VVG) and von Kossa (calcium) stain respectively. We used anti-CD34 (1:1500) for immunohistochemical staining of PCL grafts and PCL/fibrin grafts at different time periods. Images were collected and saved under an upright light microscope (NIKON ECLIPSE E100, Japan).

Briefly, the immunofluorescence test should be performed after washing the prepared frozen sections 3 times with PBS, and then 5% fetal bovine serum solution was added at room temperature for 1 h. Furthermore, infiltration was performed for 20 min using 0.2% TritonX-100 solution diluted. Simultaneously, monoclonal antibody (1:500) was added and incubated at 4 °C for 12 h. secondary antibody (1:500) was added and incubated for 1 h in a light-shielded environment. Finally, DAPI (1: 1000) solution was added at different times to stain the nuclei.

Endothelial cell staining experiments were expressed by rabbit anti-von Willebrand factor (vWF, 1:200) antibody and mouse monoclonal anti-CD34 (1:70). Vascular smooth muscle cell staining was expressed by markers of mouse anti-α-SMA (1:200) and mouse anti-SM-MHC (1:500) primary antibody. We used mouse anti-CD68 antibody (1:300) to detect the presence of inflammatory cells in the graft. Furthermore, cytokine ELISA kit was used to detect inflammation-related factors. To observe M1 and M2 macrophages, rabbit anti-iNOS antibody (1:200) and macrophage anti-mannose receptor/CD206 antibody (1:300) were used. We used Image-J software to calculate the fluorescence intensity of the characteristic factor iNOS of M1 type macrophages and the characteristic factor CD206 of M2 type macrophages in 3 parallel groups, and divided the fluorescence intensity of CD206 by the fluorescence intensity of iNOS, thereby to get the ratio of M2/M1. All pictures were collected and stored under a fluorescence microscope (Olympus BX53TR, Japan) and checked with ImageJ software.

2.9. Statistical analysis

Quantitative results in this article were taken from more than three samples. All measured results were expressed as mean ± SD. Statistical analysis was performed using OriginPro software (version 9.0, USA) and Graphpad Prism software (Version7, USA). $P < 0.05$ represented statistical significance.

3. Results

3.1. The characterization of electrospun PCL/fibrin vascular grafts

PCL and fibrin were used as raw materials to prepare vascular grafts using electrospinning technology. The schematic diagram of preparing PCL/fibrin by electrospinning was illustrated in Fig. 1A. Fig. 1B indicated a successfully fabricated PCL/fibrin tubular vascular scaffold, which had a length of 1 cm, a wall thickness of 0.2 mm and an inner diameter of 3 mm. Under the SEM, the microscopic morphology of the electrospun PCL/fibrin nanofibers was carefully observed. As it could be seen, the surface of the fibers was smooth, which had a certain porosity and was beneficial to cell adhesion, migration and proliferation (Fig. 1C–D).

3.2. Changes in the mechanical strength and degradation properties of the graft in vivo

From Fig. 2A and B, it can be seen that the grafts could be easily

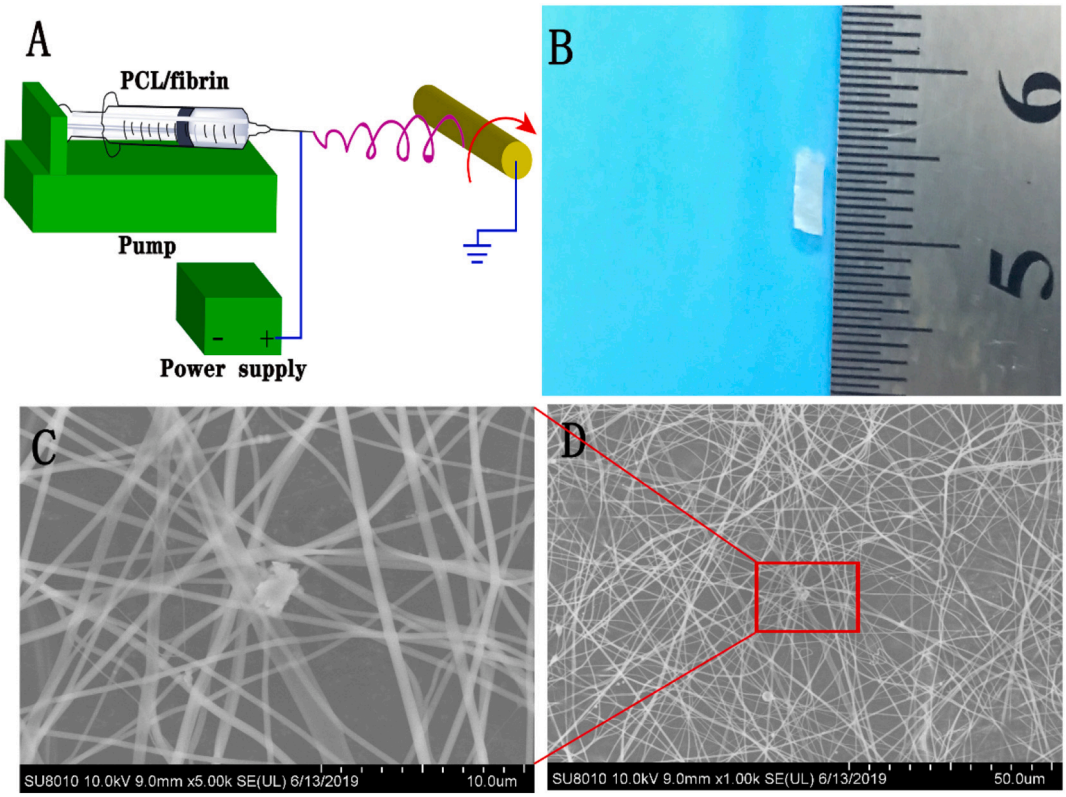

Fig. 1. Preparation and observation of PCL/fibrin vascular grafts. The schematic diagram of electrospun PCL /fibrin grafts (A), macroscopic appearances of the PCL/fibrin grafts (B). Morphology of vascular grafts was observed by SEM (C and D). Scale bars represented 10 μm in C and 50 μm in D, respectively.

distinguished from native artery at 1 and 3 months, but at 9 months vascular grafts and native artery were difficult to distinguish. Furthermore, the graft treated with 0.9% sodium chloride solution was clear and bright, almost the same as the native artery (Fig. 2B). Under the stereo microscope, it was found that the thickness and morphology of the lumen were different in different time periods, and a small amount of artery-like tissue was also seen (Fig. 2C). Interestingly, compliance of implanted PCL/fibrin grafts gradually increased at 1, 3 and 9 months successively. However, the compliance values of PCL/fibrin vascular grafts were lower than PCL vascular grafts at different time periods (Fig. 2D). In Fig. 2E–G, we also found that the breaking strain (224 ± 35.2%) of implanted PCL graft at 9 months decreased, but its maximum stress (5.97 ± 0.35 Mpa) and elastic modulus (8.31 ± 0.23 Mpa) both increased significantly, compared to the PCL control group. However, the values of breaking strain, elastic modulus and maximum stress of the PCL/fibrin graft at 9 months were similar with native artery. The elastic modulus and maximum stress of neoartery decreased significantly, compared to pre-implantation PCL/fibrin graft. Importantly, degradation performance of scaffold materials in vivo plays an important role in its mechanical strength. SEM showed that there was a small amount of cell infiltration in the PCL/fibrin fiber and the structure was relatively complete by 1 month, and part of the fiber structure was broken by 3 months. However, at 9 months the scaffold fiber degraded obviously and cells proliferated largely (Fig. 2H). Moreover, it was demonstrated that the percentage of weight retention of PCL/fibrin scaffold fiber was 89 ± 4.2% at 1 month and 35 ± 3.5% at 9 months respectively, which had statistically significant difference (Fig. 2I). Surprisingly, with the prolonged implantation time, the percentage of weight retention of PCL scaffolds was much higher than that of PCL/fibrin scaffolds.

3.3. Functional regeneration of the replaced artery by PCL/fibrin vascular grafts

The aortic ring bioassay experiments showed that the contraction strength of PCL/fibrin vascular grafts (3.4 ± 0.19 g for KCl, and 3.8 ± 0.36 g for AD) was significantly higher than that of PCL grafts (2.1 ± 0.24 g for KCl, and 2.2 ± 0.42 g for AD) under the action of vasomotor agonists. However, the contractility of native artery was best (Fig. 3A). Furthermore, under the stimulation of vasodilators, although the relaxation intensity of PCL/fibrin graft (58.4 ± 6.3% for Ach, and 52 ± 2.8% for SNP) was lower than that of PCL graft (77 ± 3.1% for Ach, and 103 ± 5.9% for SNP), it was very closed to native artery (Fig. 3B). This experiment confirmed that the graft could react with vasoactive agent, and also showed that it had excellent vasoconstriction and vasodilator function.

3.4. Endothelialization of PCL/fibrin grafts

At 9 months of in vivo transplantation, PCL grafts, PCL/fibrin grafts and native samples were respectively taken out. SEM results showed that the luminal surface of the samples was very smooth and clean, and no thrombosis and platelet aggregation were found (Fig. 4A–C). Compared with PCL grafts (Fig. 4D and G), PCL/fibrin grafts (Fig. 4E and H) showed that there were more cobblestone-like cells covering the surface, which was slightly less than the native artery (Fig. 4F and I). Here, it was emphasized that this type of cell referred to endothelial cells. The arrangement of endothelial cells paralleled with blood flow direction. To further test this conclusion, we used vWF factor and DAPI to fluorescently stain samples at 9 months. We found that the luminal surface of the PCL/fibrin graft had a continuous endothelial monolayer similar to that of native artery (Fig. 4J–O). Endothelialization coverage rate of the grafts was analyzed based on immunological images, and we found that the endothelialization coverage value of PCL/fibrin grafts

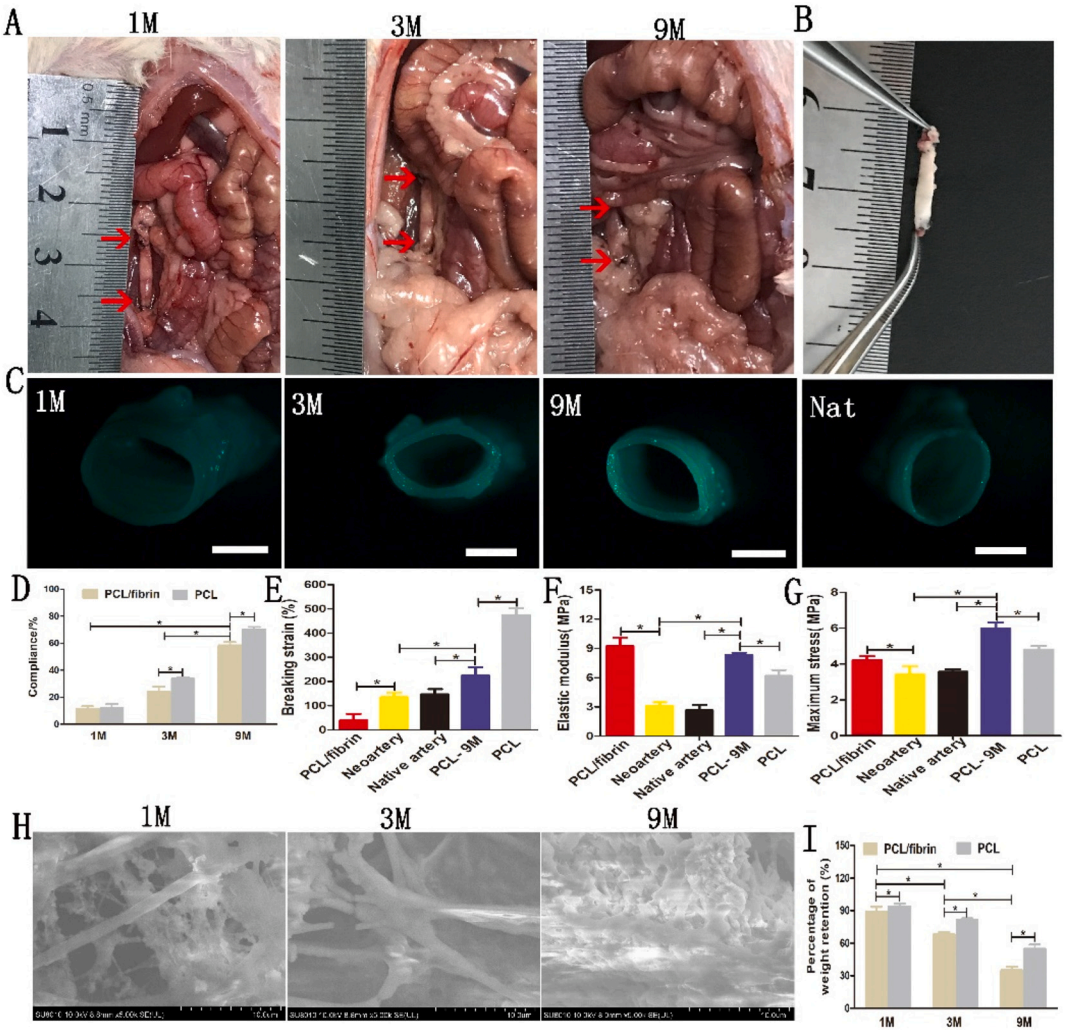

Fig. 2. Implantation into the abdominal aorta, changes in the mechanical characteristics and morphology of the electrospun graft. Macroscopic pictures of the graft at 1, 3 and 9 months after transplantation (A). The red arrow indicated the anastomotic location of vascular graft. The appearance of the graft at 9 months after treatment with physiological saline solution (B). Gross view of the cross-sections of explanted PCL/fibrin grafts after 1, 3 and 9 months (C). (D), Compliance values of PCL/fibrin and PCL vascular grafts after 1, 3, and 9 months (n = 3). The mechanical properties of the vascular graft (n = 3) indicated the breaking strain (E), elastic modulus (F) and maximum stress (G). Changes of PCL/fibrin vascular grafts at different time periods were observed with SEM (H) and the percentage of weight retention of different grafts were measured at 1, 3 and 9 months respectively (I) (n = 3). Scale bar: (C) 1 mm. *indicated P < 0.05. (For interpretation of the references to colour in this figure legend, the reader is referred to the web version of this article.)

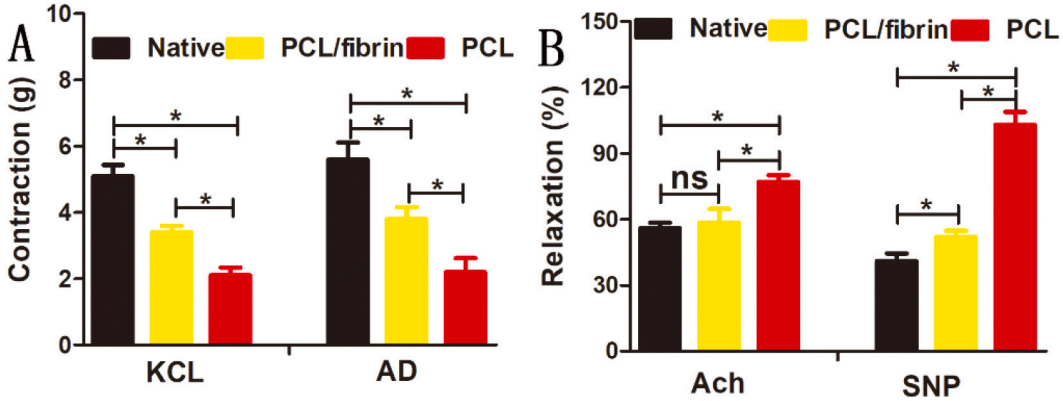

Fig. 3. Regeneration of graft vascular function after 9 months. Contraction effects of KCl and AD in native artery, PCL/fibrin graft and PCL graft (A) (n = 3); Relaxation effects of Ach and SNP (B) (n = 3). * referred to statistical significance, ns indicated no statistical significance.

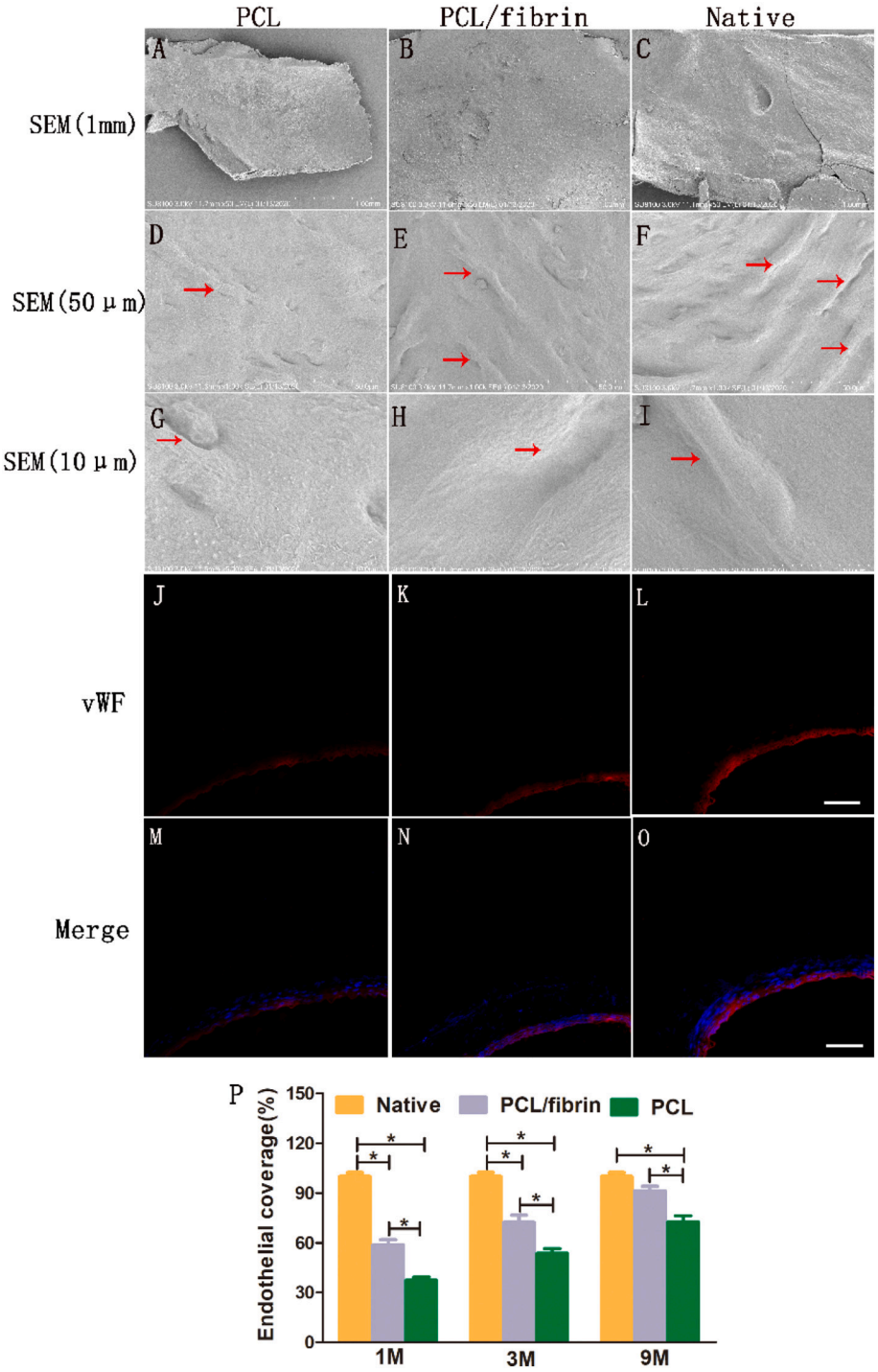

Fig. 4. General situation of endothelialization in different grafts. The general morphology of the inner layer surface of different grafts was observed by SEM at 1 mm (A, B and C), 50 μm (D, E and F), and 10 μm (G, H and I). Red arrows indicated vascular ECs. Immunofluorescence images of PCL grafts (J and M), PCL/fibrin grafts (K and N) and native artery (L and O) stained with vWF (red) and DAPI (blue), respectively. Scale bar: 100 μm. Endothelial coverage of different grafts was calculated (P) ($n = 3$). $_{*}$ $p < 0.05$. (For interpretation of the references to colour in this figure legend, the reader is referred to the web version of this article.)

was higher than that of PCL grafts at 1, 3 and 9 months, respectively, which was because fibrin had good biocompatibility and could effectively promote the proliferation of endothelial cells. As the implantation time increased, the endothelialization coverage of PCL/fibrin grafts continued to increase. At 9 months, there was no statistical difference in endothelialization coverage between PCL/fibrin grafts and native artery (Fig. 4P).

3.5. Rapid regeneration in PCL/fibrin vascular graft

HE staining results showed that the cell distribution was in a circumferential arrangement, and no residual degraded graft was found (Fig. 5B). However, electrospun PCL grafts showed fewer SMCs and thinner graft wall (Fig. 5A, E and I). At 9 months after transplantation, the wall thickness and cell number of the PCL/fibrin grafts were close to those of native artery (Fig. 5B–D). In order to test whether the regeneration of the vascular media layer was related to PCL/fibrin graft

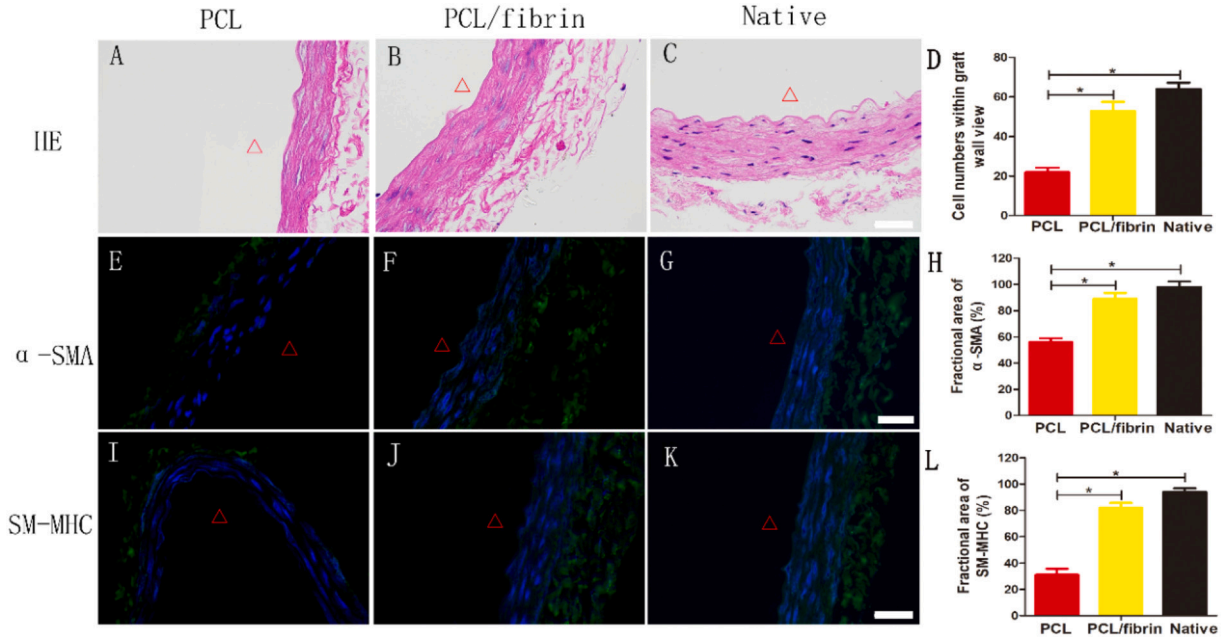

Fig. 5. Regeneration of vascular media layer within PCL/fibrin grafts at 9 months in vivo. HE stained images of different grafts after 9 months (A–C). Statistical analysis of cell numbers within graft different grafts (D) (n = 3). Distribution of VSMCs infiltration in different grafts under immunofluorescence test (α-SMA, green) (E-G). Fractional area of α-SMA within the graft (H) (n = 3). Immunofluorescence experiments of grafts with contractile VSMCs (SM-MHC, green) (I–K). Fractional area of SM-MHC within the graft (L) (n = 3). Cell nuclei were stained with DAPI (blue). Δ indicated the lumen. * represented $P < 0.05$. Scale bar: 100 μm. (For interpretation of the references to colour in this figure legend, the reader is referred to the web version of this article.)

remodeling, we used α-SMA markers to stain the grafts and view them under a fluorescence microscope. The results of immunofluorescence experiments showed that the α-SMA expression quantity in PCL/fibrin vascular grafts group was similar with native artery group (Fig. 5F–H). Late-stage differentiation of VSMCs is often marked by myosin heavy chain (SM-MHC). A higher level of SM-MHC expression was observed in PCL/fibrin graft, which indicated that the PCL/fibrin graft had contractile phonotype function (Fig. 5J). Surprisingly, only a thin smooth muscle media layer was seen in the PCL graft (Fig. 5A). The expression levels of α-SMA and SM-MHC in PCL/fibrin grafts were far higher than those in PCL grafts, which may be closely related to the fibrin contained in PCL/fibrin (Fig. 5E–L).

3.6. ECM remodeling in PCL/fibrin grafts

ECM remodeling plays a critical role in the process of vascular regeneration. In order to evaluate the composition and function of ECM, Masson, Safranin O and VVG were used respectively stained to detect the collagen, glycosaminoglycan (GAG) and elastin content of three different grafts after 9 months. It could be seen from Fig. 6 that compared with PCL grafts, compact ECM deposits were obviously present in PCL/fibrin grafts wall. Interestingly, the grafts staining results with Masson's kit showed that the fibrillar collagen in the PCL/fibrin graft was closely aligned with the periphery of the luminal and arranged in circumferential appearance. It was also found that the collagen layer of PCL/fibrin grafts were very similar to that of native artery (Fig. 6A–C). To detect the presence of GAGs in the neoartery wall, safranin O was used for verification. Compared to PCL grafts, the GAGs in PCL/fibrin grafts were located mostly on the side of the luminal and were similar to native arteries (Fig. 6E–G). Simultaneously, staining results for elastin using Verhoeff kit confirmed the presence of an elastic layer in the PCL/fibrin neoartery wall (Fig. 6I–K). Furthermore, the quantitative analysis results indicated that the collagen content in the PCL/fibrin grafts was more than that in the PCL grafts (Fig. 6D). While compared with native artery, the content of elastin and GAG were less in PCL grafts and PCL/fibrin grafts (Fig. 6H and L). Importantly, the distribution of collagen, GAG and elastin was more abundantly in PCL/fibrin graft walls, but the ECM protein (collagen, GAG and elastin) distribution was relatively scarce in PCL graft walls. This may be because PCL/fibrin could more effectively facilitate the secretion of extracellular matrix.

3.7. Analysis of vessel density and calcification in vivo

To evaluate the presence of microvessels in the graft wall, we used CD34 immunohistochemistry to stain PCL grafts and PCL/fibrin grafts at different time points. Fig. 7A–B showed that the content of cellularity and vascularization in PCL/fibrin grafts at 3 months was significantly higher than that in the PCL grafts. Brown parts represented CD34-stained microvessels. In addition, it was calculated from the CD34-stained images that vascular density value in PCL/fibrin grafts increased to 4.8 ± 0.6HPF at 1 month, and reached the highest value (12.1 ± 0.28HPF) at 3 months. Otherwise, vascular density value in the PCL/fibrin graft decreased at 9 months. At 9 months, there was no statistically significant difference in vascular density between the PCL graft and the PCL/fibrin graft. At the same time, the vascular density of PCL grafts gradually increased with the time of transplantation (Fig. 7C).

To assess the calcification in the vascular grafts, we performed von Kossa staining at 1, 3 and 9 months. The principle of graft calcification is the differentiation of smooth muscle cells into chondrocytes, resulting in chondroid metaplasia, and then the spread of chondroid metaplasia resulted in calcified areas. PCL grafts had significantly more calcification than PCL/fibrin grafts. It was also observed that the calcification site in the graft was located near the lumen (Fig. 7D–E). Graft calcification measurements revealed that the calcification area of PCL/fibrin grafts (at 1, 3 and 9 months) was significantly lower than that of PCL grafts. More interestingly, the calcification levels of the PCL/fibrin graft and the PCL graft reached the highest point at 3 months, and the calcification area values were 1.16 ± 0.23% and 5.31 ± 0.14%, respectively. There was significant statistical difference between the two groups (Fig. 7F).

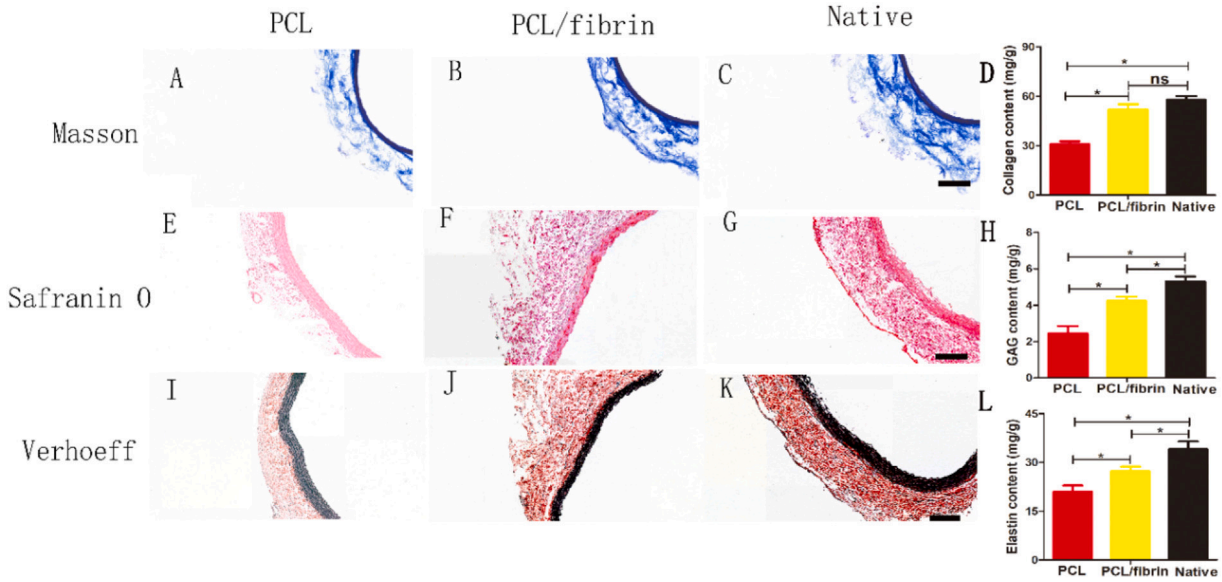

Fig. 6. Characterization of ECM deposition in 9 months after implantation. Microscopic photos of cross sections stained with Masson's for collagen (blue, A–C), safranin O for glycosaminoglycansin (red, E–G) and Verhoeff's for elastin (black, I–K) on different scaffolds. Total collagen, GAG, and elastin were assessed by corresponding detection kit respectively (D, H, L) (n = 3). Scale bar: 100 μm. * indicated statistically significant. (For interpretation of the references to colour in this figure legend, the reader is referred to the web version of this article.)

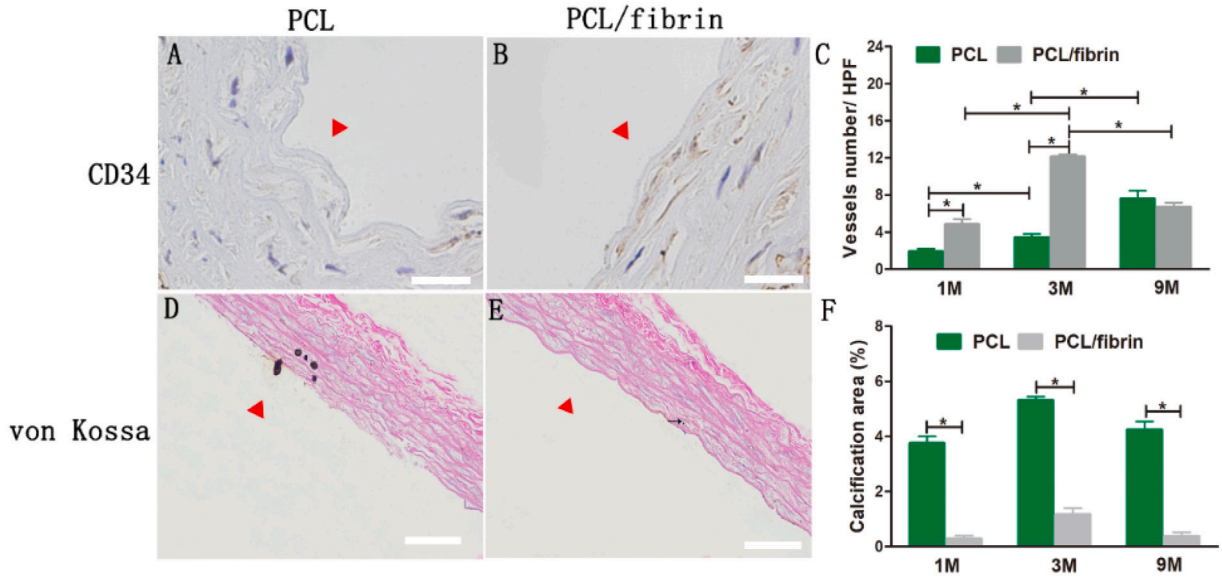

Fig. 7. Vascular density distribution and calcification in different grafts transplanted in abdominal aorta. Image of PCL graft and PCL/fibrin graft stained at 3 months with CD34 marker (A and B). Vessels numbers in PCL grafts and PCL/fibrin grafts at 1, 3 and 9 months was illustrated (C) (n = 3). Von Kossa staining of PCL/fibrin graft and PCL graft at 3 months (D–E). Black arrow indicated calcification. Calcification area ratio of grafts at different time points (F) (n = 3). Scale bar: 50 μm (A, B), 100 μm (D, E). * indicated statistical significance. Δ indicated the graft lumen.

3.8. Expression of inflammatory cytokines related to graft remodeling

Meaningless, macrophages represent an important value in vascular remodeling. As a marker for macrophages, the distribution and presence of CD68 was evaluated in vascular grafts at 1 month, 3 months and 9 months. Currently, macrophages are mainly classified into pro-inflammatory type I (M1) and anti-inflammatory type II (M2) according to different activation states, functions and secret factors [23]. As showed in Fig. 8A, the number of macrophages cells in 9 months was significantly less than that in 1 and 3 months. Immunofluorescence tests results for the graft by 9 months showed that the number of iNOS $^{+}$ cells was significantly less than that of CD206 $^{+}$ cells (Fig. 8A). It can also be observed that the expression level of iNOS decreased gradually with time prolong, but CD206 expression was still at a higher level. Compared with the expression of native arteries, both CD206 and iNOS expression were higher (Fig. 8A). ImageJ software 1.8.0 was used to calculate M2/M1 ratio of the graft. The M2/M1 ratio of PCL/fibrin grafts and PCL grafts both increased gradually with time prolong. Importantly, the M2/M1 ratio of PCL/fibrin grafts was significantly higher than that of PCL grafts at 3 months and 9 months (Fig. 8B).

Pro-inflammatory, anti-inflammatory cytokines and chemokines factors play a major role in the process of vascular remodeling. Therefore, we focused on exploring these critical factors in PCL/fibrin vascular grafts. At 9 months, the ELISA test results showed that the secretion of anti-inflammatory cytokines IL-4 and IL-10 decreased, respectively (Fig. 8C–D). TNF-α, IL-6 and IL-1β were important pro-

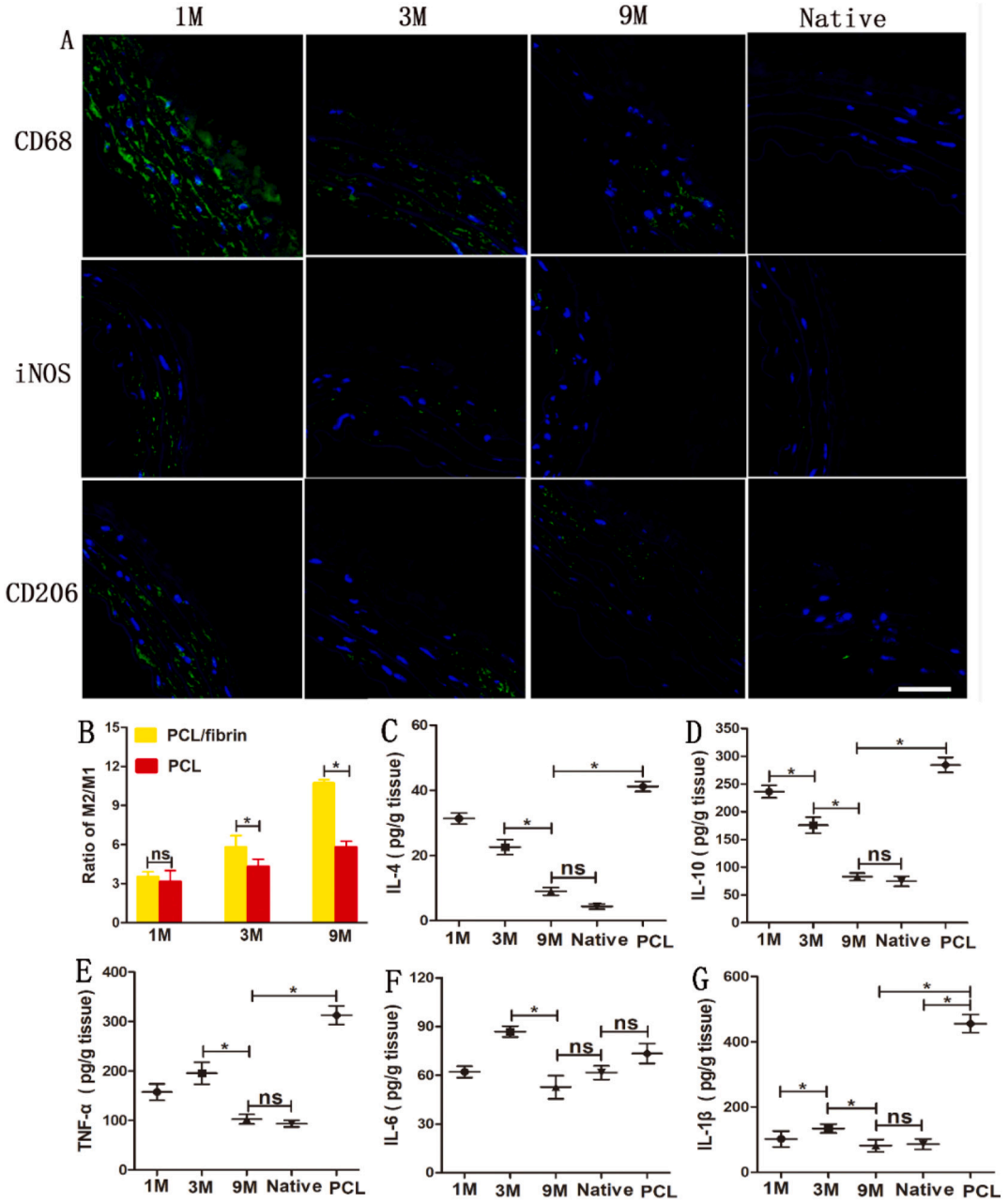

Fig. 8. Distribution of macrophages and inflammatory-related cytokines during PCL/fibrin vascular graft remodeling. CD68, iNOS and CD206 markers were fluorescently stained (green) in PCL/fibrin graft at different time periods and native artery(A). The ratio of M2/M1 macrophages in PCL/fibrin and PCL grafts (n = 3) (B). Evaluation of inflammation related cytokines IL-4 (C), IL-10 (D), TNF-α (E), IL-6 (F) and IL-1β (G) by ELISA experiments (n = 3). $P < 0.05 = {}_{*}$. ns represented no statistical significance. Scale bar: 50 μm. Blue indicated the nucleus. (For interpretation of the references to colour in this figure legend, the reader is referred to the web version of this article.)

inflammatory cytokines. The secretion amount of TNF-α was 195.4 ± 22.3 pg/g and higher, compared to 1 month. However, it was surprisingly found that TNF-α, IL-6, and IL-1β all decreased at 9 months, and eventually decreased to levels similar to the native artery (Fig. 8E–G). Interestingly, except for IL-6, all cytokines were significantly overexpressed in PCL grafts at 9 months (Fig. 8C–G).

4. Discussion

It is well known that ideal small diameter tissue engineering vascular scaffold should have highly porous structure, biodegradability, good mechanical properties, and be easy to prepare. At the same time, the scaffold should have a structure similar to native arteries, nonthrombogenicity, vasoactive, and regenerated into new functional tissue [24,25]. In addition, vascular graft that regenerates blood vessels in vivo should have the structure functions of VSMCs and ECs similar to native artery [26]. In order to design a functional tissue-engineered blood vessel, we should fabricate grafts with porous structure. In our work, PCL/fibrin tubular vascular graft was prepared by using electrospinning technology, and the high-voltage electrostatic field was used to construct a suitable fiber structure. Moreover, this preparation method can also well control the composition of the scaffold, the size of the fiber diameter, and the strength of the biomechanics [27,28]. After vascular grafts were successfully transplanted into vivo for 1, 3, and 9 months, we found that there was no thrombosis in the lumen of the graft and no intimal hyperplasia around the lumen (Fig. 2A and C).

More importantly, the morphology and structure of the neoarteries formed by the vascular graft at 9 months was very similar to the native arteries (Fig. 2B). The experimental results showed that the PCL/fibrin tubular vascular scaffold was feasible as a small diameter vascular graft. Vascular grafts are often subjected to additional forces such as compression, twisting and kinking in clinical practice. The greater the compliance, the greater the expansion of the blood vessel and the better its elasticity. The difference in compliance between vascular grafts and host the artery is the leading cause of graft failure. Therefore, we should consider the compliance index of the graft [29]. In this paper (Fig. 2D), we found that the compliance value in PCL/fibrin vascular graft gradually increased (11.5 ± 1.83% at 1 month, 24.2 ± 3.67% at 3 months, 58.4 ± 2.51% at 9 months).

The mechanical properties of functional vascular graft must be similar to that of the host blood vessel in order to maintain some functions in vivo. Simultaneously, it was found that the mechanical strength values of the neoartery and native artery were breaking strain (135 ± 18.98%) VS (147 ± 21.35%), elastic modulus (3.12 ± 0.34 Mpa) VS (2.64 ± 0.562 Mpa) and maximum stress (3.43 ± 0.425 Mpa) VS (3.57 ± 0.132 Mpa) (Fig. 2E–G). This may be due to the good biomechanical properties of PCL itself. The above results confirmed that the mechanical properties of PCL/fibrin graft could fulfill the requirements of vascular transplantation. Evaluation of vascular graft degradation performance in vivo is also a key issue that deserves attention. Wang et al. [30] results showed that PCL had a slow degradability, which led to the failure of artificial blood vessel transplantation in vivo. At present, there are still few reports on the complete degradation of PCL scaffolds, which may be because the survival time of animal models of PCL grafts is far less than the degradation time of this material [31]. However, due to the addition of fibrin, the PCL/fibrin vascular graft we prepared showed significant degradation at 9 months in this study. Furthermore, the general steps of polymer material degradation included loss of molecular weight and mass [32]. Interestingly, reduced molecular weight and fiber breakage were noted at 1, 3, and 9 months of sample transplantation.

Ideally, vascular graft should be remodeled in vivo to form a functional neoartery and it has similar function with native arteries. Allen et al. [33] fabricated a PCL/poly(glycerol sebacate) (PGS) vascular graft and implanted it into rats for 12 months. And then PCL/PGS grafts remodeled into neoarteries, which were resemble to rat native aortas. In our research, under the action of corresponding vasoactivators, native artery and PCL/fibrin graft appeared strong relaxation and contraction function, while PCL graft showed weaker performance (Fig. 3A and B). Because PCL fiber had a thicker fiber diameter, slower degradation performance and stronger stiffness, it would inhibit the function of regenerated blood vessels.

Vasoactive reactivity, mechanical strength and compliance have significant effects on the vascular media. In addition, regeneration of PCL/fibrin graft depends on whether the functional vascular media is reconstructed. Some factors such as the pore structure, composition, and mechanical function mainly affect tissue regeneration [34]. We could see that microfiber morphology of different samples arranged in a circumferential manner by H&E and immunofluorescence tests. In addition, the expression of α-SMA and SM-MHC in PCL/fibrin graft was significantly higher than that in PCL graft at 9 months respectively, but it was slightly lower than that in the native artery (Fig. 5). These results indicated that the graft successfully achieved phenotypic conversion of VSMCs in vivo, and also demonstrated that the neoartery had significant vascular activity in VSMCs. Thus, we believed that PCL/fibrin tubular scaffold could give satisfactory results for tissue regeneration.

The endothelial layer of the graft with a complete architecture and function can often effectively reduce the formation of thrombus and the proliferation of VSMCs, thereby preventing the formation of intimal hyperplasia. Researchers have continuously tried various strategies to optimize the endothelialization of small diameter vascular grafts. Wu et al. [35] used PCL as a raw material and successfully prepared a new type of nanofiber-oriented tubular scaffold through electrostatic spinning technology. The results confirmed that the scaffolds arranged by the circumferential nanofibers could promote the directional proliferation and adhesion of ECs. In our work, the PCL/fibrin graft showed endothelialization at 1 month, and the cobblestone-shaped endothelial cells in the PCL/fibrin graft were not significantly different from the native artery at 9 months (Fig. 4). Both PCL/fibrin vascular graft and native artery showed complete endothelialization after 9 months, while PCL graft had only thin layer of endothelial cell layer. This result indicated that the microstructure of PCL/fibrin grafts had significant impact on the proliferation of endothelial cells since the early stage, and its endothelialization degree was significantly higher than that of PCL grafts. This phenomenon may be because the PCL/fibrin graft was a hydrophilic composite material, which promoted endothelial cell adhesion and proliferation behavior.

How to keep the neoarteries in line with the mechanical properties of native arteries is a major problem in the field of tissue regeneration medicine. Extensive research has found that effective improvements in ECM deposition including elastin, collagen and GAG can greatly enhance mechanical strength of vascular graft. Moreover, these constituents are vital for maintaining the function of blood vessels [36,37]. We concluded that PCL grafts showed limited ECM deposition at 9 months of transplantation in SD rats. However, the collagen, GAG, and elastin in PCL/fibrin grafts neatly arranged circumferentially. More importantly, the content and arrangement structure of these ECM components were not much different from the native artery (Fig. 6). Therefore, the mechanical strength of the PCL/fibrin graft was very similar to that of native artery. We speculated that the undegraded fibers in the PCL/fibrin scaffold played a strong role in mechanical properties together with the deposition of ECM. As a result, the neoartery could withstand corresponding the impact of blood flow.

Cell infiltration is an important step in tissue regeneration. Moreover, cell proliferation, migration and infiltration depend on the internal structure of the fibers in the synthetic material and the effects of pore size [38]. In the construction of tissue engineering blood vessel, a large number of functional microvessels are needed, and the remodeling of degradable scaffolds by microvessels ingrowth is also important phenomenon which we cannot ignore. In this study, microvessels density of PCL/fibrin grafts was significantly higher than that of PCL grafts at 1 and 3 months (Fig. 7A–C). We speculated that the microstructure of PCL/fibrin vascular scaffold could effectively promote the formation of microvessels, which may be due to existence of fibrin with good biocompatibility. Nonetheless, the dense structure of PCL grafts prevented cell infiltration. Furthermore, the microvessels density values of the two groups of grafts were approximately equal at 9 months.

The issue of graft calcification always plagues researchers, so the problem is worthy of our continuous exploration. To evaluate the role of graft pore size in the development of calcifications, Tara et al. [39] experimentally showed that compared with small pore grafts, large pore grafts had well-organized neointima formation and less calcific deposition. In our study, PCL/fibrin grafts (at 1, 3, and 9 months) showed significantly less calcification areas than PCL grafts (Fig. 7D–F). We thought it was possible that the PCL/fibrin graft had a high pore structure and good biocompatibility, which effectively slowed down the formation of calcification. Furthermore, prolonged foreign body stimulation induced the production of related inflammatory cells, which was closely related to mineral deposition and eventually led to calcification. Thus, in order to hinder calcification, it was necessary to improve biocompatibility of scaffold materials.

In recent years, research generally believes that reasonable inhibition of related inflammatory reactions can effectively control infection and reduce the incidence of tissue necrosis, and its ultimate purpose is to promote tissue regeneration and healing. Until now, despite the continuous efforts of researchers to specialize in scaffold materials to achieve ideal vascular function, the vascular reconstruction of grafts is

still a huge challenge for us [40]. Members of our team also examined the presence of inflammatory responses when the remodeling of PCL/fibrin grafts was analyzed. Among them, macrophages may also be the main participants and leaders. We observed many macrophages oriented with microfibers of PCL/fibrin grafts at 1 month, and there were many CD68 positive markers. However, as the transplantation time prolonged, the $CD68^+$ macrophages gradually decreased, and by 9 months, their number was close to the native arteries (Fig. 8A). In addition, the M2/M1 ratio of macrophages in the PCL/fibrin vascular graft at 1 month was slightly larger than that of PCL graft, but it was more than PCL graft at 3 and 9 months (Fig. 8B). These results indicated that the macrophage proliferation in early stage may be caused by the topological phenomenon of the graft. As the transplantation time increased, the mechanical and degradation properties of the graft in vivo changed, which ultimately resulted in a change in the macrophage phenotype. Although the expression of different types of cytokines changes over time, the expression of anti-inflammatory cytokines had relations with that of pro-inflammatory cytokines. At 9 months, the expression of different cytokines in PCL/fibrin vascular grafts was not different from that of native arteries, which indicated that anti-inflammatory cytokines and pro-inflammatory cytokines interacted in vascular remodeling to obtain the best results. The interesting finding was that the expression of anti-inflammatory cytokines and pro-inflammatory cytokines of PCL/fibrin vascular grafts was significantly less than that of PCL grafts at 9 months (Fig. 8C–G). We speculated that PCL grafts had slow degradation properties and poor biocompatibility, which prolonged the continuous appearance of inflammation.

5. Conclusion

In this paper, we used electrospinning technology to prepare a circumferentially arranged tubular vascular graft, and confirmed that the mechanical properties and vascular function of the PCL/fibrin graft were similar to native arteries by experiments in vivo. Meanwhile, compared to the PCL graft, PCL/fibrin graft showed a higher level of expression of smooth muscle contractile protein after 9 months, improved ECM deposition, rapid endothelialization, reasonably regulated macrophage expression and rare presence of calcifications. To sum up, these data indicated that PCL/fibrin vascular grafts could induce the host to perform functional reconstruction and vascular regeneration, which laid the foundation for the development of small diameter tissue engineering blood vessel.

CRediT authorship contribution statement

Conception and design: Qiqing Zhang, Yuzhen Dong, Liang Zhao.

Analysis and interpretation: Lei Yang, Hongli Chen, Changhong Zhao.

Data collection: Lei Yang, Lulu Sun, Fengyao Wang, Rui Zhang.

Writing the article: Liang Zhao, Lei Yang, Xiafei Li.

Critical revision of the article: Chengqiang Yang, Haibin Zong.

Final approval of the article: Liang Zhao, Qiqing Zhang, Yuzhen Dong.

Statistical analysis: Lei Yang, Shicheng Wang, Xiafei Li, Shuang Song, Qiong Li, Songfeng Mu.

Overall responsibility: Liang Zhao, Qiqing Zhang.

Declaration of competing interest

The authors declare that they have no known competing financial interests or personal relationships that could have appeared to influence the work reported in this paper.

Acknowledgement

In this work, we have received strong financial support by the National Natural Science Foundation of China (81901874, 81903164), Zhengzhou Key Laboratory of Cardiac Structure Research (2019KFKT006), Postgraduate Research and Innovation Support Plan Project of Xinxiang Medical University (YJSCX201905Z), the College Student Innovation and Entrepreneurship Training Program Project of Henan Province (141039, 110411), Research and Innovation of College Students in Xinxiang Medical University (xyxskyz201948), Science and Technology Research Project (social development) of Henan Province in 2018 (182102310067), Independent Research Fund of Beijing in 2019, Plateau Discipline (Surgery) of the First Clinical College of Xinxiang Medical University, Opening Project Fund of Henan Key Laboratory of Neurological Repair (HNSJXF-2016-011), Novel Coronavirus Pneumonia Research and Development Project in 2020 of Medical Engineering College in Xinxiang Medical University (XYYXGC2020–005).

References

[1] E.J. Benjamin, S.S. Virani, C.W. Callaway, A.M. Chamberlain, A.R. Chang, S. Cheng, S.E. Chiuve, M. Cushman, F.N. Delling, R. Deo, S.D. de Ferranti, J.F. Ferguson, M. Fornage, C. Gillespie, C.R. Isasi, M.C. Jimenez, L.C. Jordan, S.E. Judd, D. Lackland, J.H. Lichtman, L. Lisabeth, S. Liu, C.T. Longenecker, P.L. Lutsey, J.S. Mackey, D.B. Matchar, K. Matsushita, M.E. Mussolino, K. Nasir, M. O'Flaherty, L.P. Palaniappan, A. Pandey, D.K. Pandey, M.J. Reeves, M.D. Ritchey, C.J. Rodriguez, G.A. Roth, W.D. Rosamond, U.K.A. Sampson, G.M. Satou, S.H. Shah, N.L. Spartano, D.L. Tirschwell, C.W. Tsao, J.H. Voeks, J.Z. Willey, J.T. Wilkins, J.H. Wu, H.M. Alger, S.S. Wong, P. Muntner, Heart disease and stroke statistics-2018 Update: a report from the American Heart Association, Circulation 137 (12) (2018) e67–e492.

[2] F.M. Wekesah, C. Kyobutungi, D.E. Grobbee, K. Klipstein-Grobusch, Understanding of and perceptions towards cardiovascular diseases and their risk factors: a qualitative study among residents of urban informal settings in Nairobi, BMJ Open 9 (6) (2019) e026852.

[3] V.N. Jaspan, G.L. Hines, The current status of tissue-engineered vascular grafts, Cardiol. Rev. 23 (5) (2015) 236–239.

[4] R.Y. Kannan, H.J. Salacinski, P.E. Butler, G. Hamilton, A.M. Seifalian, Current status of prosthetic bypass grafts: a review, J Biomed Mater Res B Appl Biomater 74 (1) (2005) 570–581.

[5] T. Sologashvili, S.A. Saat, J.C. Tille, S. De Valence, D. Mugnai, J.P. Giliberto, J. Dillon, A. Yakub, Z. Dimon, R. Gurny, B.H. Walpoth, M. Moeller, Effect of implantation site on outcome of tissue-engineered vascular grafts, Eur. J. Pharm. Biopharm. 139 (2019) 272–278.

[6] N. L'Heureux, N. Dusserre, A. Marini, S. Garrido, L. de la Fuente, T. McAllister, Technology insight: the evolution of tissue-engineered vascular grafts—from research to clinical practice, Nat. Clin. Pract. Cardiovasc. Med. 4 (7) (2007) 389–395.

[7] R.D. Sayers, S. Raptis, M. Berce, J.H. Miller, Long-term results of femorotibial bypass with vein or polytetrafluoroethylene, Br. J. Surg. 85 (7) (1998) 934–938.

[8] D. Pankajakshan, D.K. Agrawal, Scaffolds in tissue engineering of blood vessels, Can. J. Physiol. Pharmacol. 88 (9) (2010) 855–873.

[9] M. Agko, E.W. Liu, T.C.T. Huang, F. Lo Torto, P. Ciudad, O.J. Manrique, H.C. Chen, The split vein graft "splint" to avoid kinking and compression of the vascular pedicle, Microsurgery 37 (6) (2017) 739–740.

[10] N.R. Patel, M. Bole, C. Chen, C.C. Hardin, A.T. Kho, J. Mih, L. Deng, J. Butler, D. Tschumperlin, J.J. Fredberg, Cell elasticity determines macrophage function, PLoS One 7 (9) (2012) e41024.

[11] R. Sridharan, A.R. Cameron, D.J. Kelly, C.J. Kearney, F.J. O'Brien, Biomaterial based modulation of macrophage polarization: a review and suggested design principles, Mater. Today 18(6) 313–325.

[12] W.F. Liu, C.M. Nelson, J.L. Tan, C.S. Chen, Cadherins, RhoA, and Rac1 are differentially required for stretch-mediated proliferation in endothelial versus smooth muscle cells, Circ. Res. 101 (5) (2007).

[13] J. Qiu, Y. Zheng, J. Hu, D. Liao, H. Gregersen, X. Deng, Y. Fan, G. Wang, Biomechanical regulation of vascular smooth muscle cell functions: from in vitro to in vivo understanding, J. R. Soc. Interface 11 (90) (2014) 20130852.

[14] P. Zilla, D. Bezuidenhout, P. Human, Prosthetic vascular grafts: wrong models, wrong questions and no healing, Biomaterials 28 (34) (2007) 5009–5027.

[15] A.A. Ksiazek, L. Frese, P.E. Dijkman, B. Sanders, Puncturing of lyophilized tissue engineered vascular matrices enhances the efficiency of their recellularization, Acta Biomater. 15 (71) (2018) 474–485.

[16] L. Chung, D.R. Maestas, F. Housseau, J.H. Elisseeff, Key players in the immune response to biomaterial scaffolds for regenerative medicine, Adv. Drug Deliv. Rev. 114 (2017) 184–192.

[17] I. Javaid, O. Yoshinobu, O. John, A. Alexandre, W. Ron, S. Patrick, Bioresorbable scaffolds: rationale, current status, challenges, and future, Eur. Heart J. 12 (2013) 765–776.

[18] C.E. Schmidt, J.M. Baier, Acellular vascular tissues: natural biomaterials for tissue

repair and tissue engineering, Biomaterials 21 (2000) 2215–2231.
[19] L. Yang, X. Li, D. Wang, S. Mu, W. Lv, Y. Hao, X. Lu, G. Zhang, W. Nan, H. Chen, L. Xie, Y. Zhang, Y. Dong, Q. Zhang, L. Zhao, Improved mechanical properties by modifying fibrin scaffold with PCL and its biocompatibility evaluation, J. Biomater. Sci. Polym. Ed. (2020) 1–21.
[20] Z. Liang, Y. Xu, H. Meng, W. Zhang, L. Min, Preparation of spider silk protein bilayer small-diameter vascular scaffold and its biocompatibility and mechanism research, Compos. Interfaces 21 (9) (2014) 869–884.
[21] L. Zhao, D. Chen, Q. Yao, M. Li, Studies on the use of recombinant spider silk protein/polyvinyl alcohol electrospinning membrane as wound dressing, Int. J. Nanomedicine 12 (2017) 8103–8114.
[22] L. Zhao, Y.L. Xu, M. Li, Y.Q. Chen, Preparation of bilayer spider silk protein vascular scaffold and its biomechanical properties and cell compatibility, J. Med. Biomech. 28 (5) (2013) 559–566.
[23] S.W. Chensue, J.H. Ruth, K. Warmington, P. Lincoln, S.L. Kunkel, In vivo regulation of macrophage IL-12 production during Type 1 and Type 2 cytokine-mediated granuloma formation, J. Immunol. 155 (7) (1995) 3546–3551.
[24] D.W. Hutmacher, Scaffold design and fabrication technologies for engineering tissues — state of the art and future perspectives, J. Biomater. Sci. Polym. Ed. 12 (1) (2001) 107–124.
[25] S.J. Hollister, Porous scaffold design for tissue engineering, Nat. Mater. 4 (7) (2005) 518–524.
[26] M. Zhu, Z. Wang, J. Zhang, L. Wang, X. Yang, J. Chen, G. Fan, S. Ji, C. Xing, K. Wang, Q. Zhao, Y. Zhu, D. Kong, L. Wang, Circumferentially aligned fibers guided functional neoartery regeneration in vivo, Biomaterials 61 (2015) 85–94.
[27] B.W. Tillman, S.K. Yazdani, S.J. Lee, R.L. Geary, A. Atala, J.J. Yoo, The in vivo stability of electrospun polycaprolactone-collagen scaffolds in, vascular reconstruction, Biomaterials 30 (4) (2009) 583–588.
[28] D.D. Swartz, J.A. Russell, S.T. Andreadis, Engineering of fibrin-based functional and implantable small-diameter blood vessels, J. Vasc. Surg. 43 (4) (2006) 867-867.
[29] S.Y. Horng, C.-K. Chen, C.-H. Lee, S.-L. Horng, Quantitative relationship between vascular kinking and twisting, Ann. Vasc. Surg. 24 (8) (2010) 1154–1155.
[30] Z. Wang, Y. Cui, J. Wang, X. Yang, Y. Wu, K. Wang, X. Gao, D. Li, Y. Li, X.-L. Zheng, The effect of thick fibers and large pores of electrospun poly(ε-caprolactone) vascular grafts on macrophage polarization and arterial regeneration, Biomaterials 35 (22) (2014) 5700–5710.
[31] H. Sun, L. Mei, C. Song, X. Cui, P. Wang, The in vivo degradation, absorption and excretion of PCL-based implant, Biomaterials 27 (9) (2006) 1735–1740.
[32] NA, Biomaterials science: an introduction to material in medicine, J. Clin. Eng. 22 (3) (1997) 154.
[33] R.A. Allen, W. Wu, M. Yao, D. Dutta, X. Duan, T.N. Bachman, H.C. Champion, D.B. Stolz, A.M. Robertson, K. Kim, Nerve regeneration and elastin formation within poly(glycerol sebacate)-based synthetic arterial grafts one-year post-implantation in a rat model, Biomaterials 35(1) 165–173.
[34] T.U. Nguyen, C.A. Bashur, V. Kishore, Impact of elastin incorporation into electrochemically aligned collagen fibers on mechanical properties and smooth muscle cell phenotype, Biomed. Mater. 11 (2) (2016) 025008.
[35] H. Wu, J. Fan, C.-C. Chu, J. Wu, Electrospinning of small diameter 3-D nanofibrous tubular scaffolds with controllable nanofiber orientations for vascular grafts, 21(12) 3207–3215.
[36] R. Gauvin, M. Guillemette, T. Galbraith, J.M. Bourget, D. Larouche, H. Marcoux, D. Aube, C. Hayward, F.A. Auger, L. Germain, Mechanical properties of tissue-engineered vascular constructs produced using arterial or venous cells, Tissue Eng. A 17 (15–16) (2011) 2049–2059.
[37] M. Baguneid, A. de Mel, L. Yildirimer, B.J. Fuller, G. Hamilton, A.M. Seifalian, In vivo study of a model tissue-engineered small-diameter vascular bypass graft, Biotechnol. Appl. Biochem. 58 (1) (2011) 14–24.
[38] B.H. Walpoth, G.L. Bowlin, The daunting quest for a small diameter vascular graft, Expert Rev. Med. Devices 2 (6) (2005) 647–651.
[39] S. Tara, H. Kurobe, K.A. Rocco, M.W. Maxfield, C.A. Best, T. Yi, Y. Naito, C.K. Breuer, T. Shinoka, Well-organized neointima of large-pore poly(l-lactic acid) vascular graft coated with poly(l-lactic-co-ε-caprolactone) prevents calcific deposition compared to small-pore electrospun poly(l-lactic acid) graft in a mouse aortic implantation model, Atherosclerosis 237 (2) (2014) 684–691.
[40] K.L. Spiller, T.J. Koh, Macrophage-based therapeutic strategies in regenerative medicine, Adv. Drug Deliv. Rev. 122 (2017) 74–83.